PHYSICAL REVIEW B VOLUME 27, NUMBER 6 15 MARCH 1983

Surface-atom x-ray photoemission from clean metals: Cu, Ag, and Au

P. H. Citrin and G. K. Wertheim
Bell Laboratories, Murray Hill, New Jersey 07974

Y. Baer
Department of Physics, University of Neuchâtel, CH-2000 Neuchâtel, Switzerland
(Received 5 August 1982)

Surface-atom core-level shifts from evaporated noble metals are reported using angle-dependent x-ray photoemission with monochromatized Al$K\alpha$ radiation. The absence of line broadening with increasing takeoff angle for the case of aluminum metal, where the surface shift is known to be small, confirms that the shifts observed in the noble metals are real surface phenomena. An analysis procedure is developed which establishes that the effect of the vacuum-solid interface in these systems is confined to the first atomic layer. The asymmetric (final-state–related) line shapes of the surface- and bulk-atom photopeaks are also shown to be identical within experimental error. The surface core-level shifts are -0.40 ± 0.02 eV for Au, -0.08 ± 0.03 eV for Ag, and -0.24 ± 0.02 eV for Cu, with the surface contributions occurring at lower electron binding energy. The analysis additionally yields electron mean free paths of 19 ± 3 Å at 1400 eV in Au and 14 ± 3 Å at 550 eV in Cu. Using the surface-to-bulk intensity ratios of the Au $4f$ core levels, it was possible to isolate the contribution of the surface-atom valence electrons. The width of the surface density of states is narrowed $(8\pm2)\%$ with respect to the bulk density of states and its center of gravity is shifted by -0.5 ± 0.1 eV. The analysis procedures and conclusions presented here should be applicable to core and valence surface-atom photoemission from a wide variety of other systems.

I. INTRODUCTION

For over a decade it has been known[1–3] that most photoemission measurements contain an appreciable contribution of electrons originating from the surface because escape depths of $\sim$10–1500-eV electrons are only a few monolayers. Understandably, interpretations of core and valence photoemission spectra based solely on bulklike properties have elicited skepticism because the surface-atom contributions could well be different. Such criticism has generally been met with the counterargument that since bulk theory and experiment tend to agree, the surface contribution must be small or indistinguishable from the bulk. On this belief any disagreement between theory and experiment is then attributed to inadequacies of the bulk theory. Others not content with these arguments have continued an active search for manifestations of surface effects in the data. Could the surface contribution be too small, or too poorly resolved, or otherwise indistinguishable from the bulk? Since surface atoms have fewer neighbors than bulk atoms, the surface valence-band width, which reflects the degree to which the electrons are delocalized, *should* be narrower than that of the bulk. Furthermore, because the "chemical" environment is different at the surface, the core-electron binding energies of the surface atoms must be different from those of the bulk. This *should* be reflected in a "chemically shifted" core-level component. Since the surface layer must contribute significantly to the measured spectrum due to the small photoemitted electron escape depths, these effects, if sufficiently large, *should* be readily observable.

Numerous early attempts to detect such differences between surface- and bulk-atom photoemission have led to conflicting or negative results. Houston *et al.*[4] claimed to have observed surface-atom core-level shifts in Ti, Cr, and Ni by comparing surface-sensitive appearance potential spectroscopy binding energies with those obtained from hard x-ray photoemission spectra (XPS). Subsequent measurements by Webb and Williams[5] disputed those results. Mehta and Fadley[6] have observed d-band narrowing in Cu using Al$K\alpha$ radiation (1.49 keV) by enhancing the surface sensitivity of their measurements with grazing electron emission. Chye *et al.*,[7] using photon energies of 80–180 eV to enhance the sur-

face sensitivity, found no such effect in Au. Contrary to the expectations of numerous investigators (many of whom have not published their negative findings), no surface-atom core-level shifts were observed in photoemission studies of W,[8,9] Ru,[8,10] Cu,[6] Au,[11] or Al, Ni, and In.[12]

The unambiguous identification of a surface-atom core-level shift (SCS) in Au has been previously reported by us.[13] In that work we also reported the measurement of a narrowed and shifted surface density of states (DOS) for that material. We further proposed a model which relates the shifted and narrowed surface DOS to the sign and magnitude of the SCS and which elucidates its chemical dependence in Cu and Ag. Since that study a number of experimental and theoretical reports on the existence and interpretation of surface-atom core-level shifts in other metals have appeared. In the present work we elaborate on our specific results for Au and then present our study of the core-level spectra from Cu and Ag. The data analysis procedures developed for all the noble metals are described in considerable detail because the bulk and surface components are not well resolved. Our procedures are quite general and are intended to establish the criteria for analyzing and interpreting core and valence surface-atom photoemission in other systems as well. Discussion and comparison of related studies with the present work are given in the following paper.[14]

In our assessment of the quality of fits to the data we pay particular attention to the residuals. These should contain only the statistical fluctuations of the individual data points provided the model function is capable of representing the data. When the residuals do contain additional nonrandom fluctuations it is a clear indication that the model function used in the fits is inadequate and that little significance can be attached to the parameters obtained by the least-squares adjustment. We also point out that the core-level data presented here are not subjected to a background subtraction prior to analysis. This common practice applied over a narrow range of energies is fundamentally incorrect[15] and generally makes it impossible to obtain statistically acceptable fits with physically meaningful line-shape parameters. The presence of such a background in the data was, in fact, tested by including it in a model function with its amplitude left as a free parameter. As expected, least-squares adjustment reduced it to a negligible value.

For the case of Cu and Ag metals the SCS was found to be only a small fraction of the corresponding core-hole-state lifetime width. The essential innovation which made it possible to extract the surface-atom signal from such data was the simultaneous fitting of the data for all takeoff angles. In this procedure any parameters required to have the same value in all data sets are automatically restricted to a single value. This then allows the interpretation of takeoff-angle-dependent broadening or shifts to be made in terms of bulk and surface components exclusively.

The results presented here for the noble metals serve as a starting point for understanding the nature of surface-atom photoemission in general. The following paper[14] considers our results in this general context by elaborating on our previously proposed model[13] and extending it to the other metals in the Periodic Table. In doing so, we explain why surface-atom effects have gone unobserved for so long and what further insight is to be gained from studying the details of such effects in these and other systems.

II. EXPERIMENTAL PROCEDURES AND RESULTS

Ultrapure Au, Ag, and Cu were evaporated onto cooled ($\sim 10\,^{\circ}\mathrm{C}$) optically flat glass substrates at a base pressure of $\sim 1\times 10^{-11}$ Torr, forming randomly ordered polycrystallites of $\leq 1\ \mu$m grain size[16] in films > 1000 Å thick. The films were prepared in the sample chamber of a AEI instrument, which was modified[17] to utilize monochromatic Al $K\alpha$ radiation. The total instrumental response function was determined to be very Gaussian with a full width at half maximum (FWHM) value of <0.24 eV.[17] This relatively high energy resolution for XPS with Al $K\alpha$ radiation proved to be essential for these experiments. Core- and valence-level spectra were taken as a function of takeoff angle θ, measured from the surface normal and accurate to $\pm 2°$.

Figure 1 shows the raw x-ray photoemission spectra of the narrowest (longest-lived) core levels in Au, Ag, and Cu recorded at different values of θ and normalized in peak height. A monotonically increasing shoulder on the low-binding- (high-kinetic-) energy side of the peak with increasing θ is obvious for the Au $4f_{7/2}$ level. The effect is less apparent between the normal and grazing emission spectra of the comparatively broader Cu $2p_{3/2}$ and the narrow Ag $3d_{5/2}$ levels, although an intensity enhancement on the low-binding-energy side is still in evidence. To check for the possible contribution of such asymmetric broadening from the instrumental response function we also measured normal and grazing photoemission from the very narrow Al $2p$ levels, see Fig. 1. The ultrapure Al films were prepared as above for the noble metals. Inspection of the Al $2p$ data clearly shows that the shoulder in the noble metals is not an experimental artifact. On the basis of the increasing intensity of the shoulder with in-

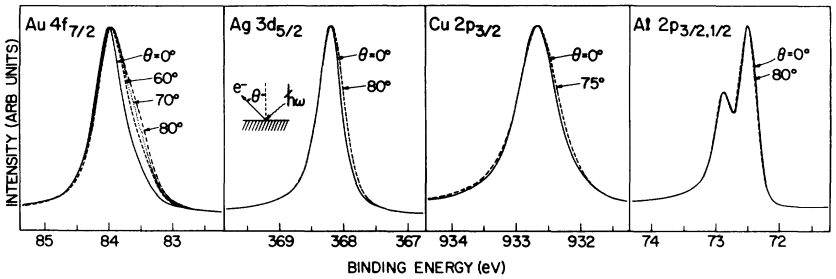

FIG. 1. Normalized x-ray photoemission spectra from evaporated films of Au, Ag, Cu, and Al as a function of increasing surface sensitivity (increasing θ).

creasing surface sensitivity (increasing θ) we assign its origin to photoemission from a surface layer.

Given that we are directly measuring surface-atom core-level photoemission we face the question of the properties of the surface photopeak, i.e., its line shape, intensity, and position, as well as the atom thickness of the region which produces the surface signal. Detailed knowledge of these properties is necessary for an understanding of surface photoemission measurements in general: How do the surface core-level spectra relate to the surface density of state? What is the role of final-state relaxation processes in determining the measured core-level binding energy? What further information could be gained by surface core and valence photoemission studies of this type in other systems?

In this section we address the characterization of the surface photoemission spectral properties in Au, Ag, and Cu. We also analyze the normal and grazing emission Al $2p$ spectra in some detail. Implications of these results in terms of the more general questions posed above are discussed in the following paper.[14]

A. Gold

We start our analysis of the Au $4f_{7/2}$ data without *a priori* knowledge regarding the number of experimentally resolvable atom-layer components in a given core-level spectrum. For simplicity we initially *assume* that the data contain only two components, corresponding to emission from bulk- and surface-atom layers. If that is true, then linear combinations of two raw (non-normalized) spectra recorded at different takeoff angles can be used to separate the individual bulk and surface contributions. This procedure is illustrated in Fig. 2. We in-

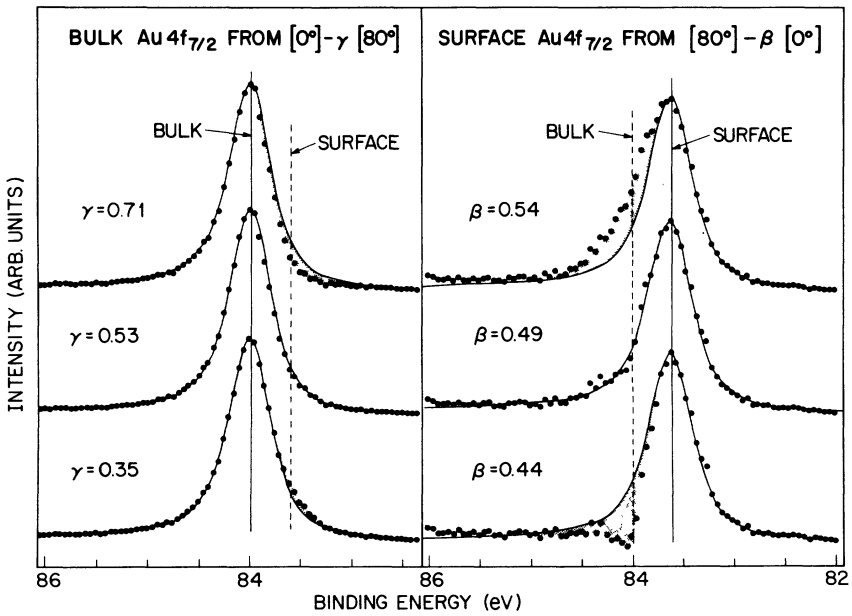

FIG. 2. Separation of bulk and surface components from the difference between $\theta=0°$ and 80° spectra. β and γ are weighting coefficients. The solid line is the Doniach-Šunjić line shape.

voke the following criteria to determine the appropriate weighting coefficients, β and γ, for the two spectra taken at $\theta=0°$ and $\theta=80°$.

(a) The line shape on the low-binding-energy side of both the surface and the bulk components must be the convolution of a Lorentzian due to lifetime broadening, a Gaussian due to photon broadening, and the instrumental response function.[15]

(b) The Au $4f$ hole-state lifetime is dominated by intra-atomic Auger processes,[18] and the photon broadening in Au (Ref. 19) is smaller than the instrumental resolution. Therefore, the low-binding-energy sides of the surface and bulk components (even if they were to have somewhat different phonon broadening) must have nearly the same shape.

(c) The high-binding-energy side of the surface component must be physically reasonable, i.e., it should not contain kinks or other pathological features.

Note that these criteria have been previously established and are unrelated to our hypothesis that there are only two components in the data.

The separation of the surface component is shown in the right-hand panel of Fig. 2. As expected, we see that independent of the coefficient β, the lower-binding-energy side of the surface line shape remains unchanged. The higher-binding-energy side, however, is seen to depend quite sensitively on β (to within $\pm 10\%$ of its value). For $\beta=0.44$ too much of the $\theta=0°$ data is subtracted from the $\theta=80°$ data and an unphysical kink results, while for $\beta=0.54$ too little 0° data is subtracted as indicated by a small kink and an unphysical additional intensity (the solid line will be explained shortly).

The lower-binding-energy side of the surface component serves as a template for the same side of the bulk component, shown separated from the surface component in the left-hand panel of Fig. 2. Near the value of $\gamma=0.53$ the right-hand side line shapes of the surface and bulk components agree, although the ability to detect very small contributions from the surface is clearly less sensitive to the choice of γ than is the corresponding ability to detect very small contributions from the bulk to the surface component with changing β. Within as much as $\pm 20\%$ of the value for γ the high-binding-energy side of the bulk component remains virtually unchanged, indicating that the residual surface component in the $\theta=0°$ data has little influence in this region.

Having separated the bulk and surface components, we now take the bulk spectrum and find *empirically* that it is fitted extremely well with a Doniach-Šunjić (DS) line shape,[20] shown as a solid line in Fig. 2. Such a line shape is characterized by the hole-state lifetime Γ and the singularity index α, which describes the partial scattering phase shifts due to the creation of electron-hole pairs. While this result for the bulk component may not seem too surprising based on similar earlier findings,[21] it is not at all obvious that the same line shape should fit the surface component equally well, see Fig. 2. The significance of this result is that using the criteria mentioned above and assuming only two components in the data we have shown that *the surface and bulk components have virtually indistinguishable DS line shapes.* Furthermore, we see from the shaded regions and the vertical solid and dashed lines shown in Fig. 2 that any misfit between the DS line shape and the difference spectrum resulting from an incorrect weighting coefficient lies almost exactly in the vicinity of the corresponding surface and bulk component peaks. This then suggests that our hypothesis that the data contain only two components is quite reasonable. Finally, we note that all the above information has been obtained simply by taking conventional difference spectra and then *empirically* fitting the results. No elaborate fitting procedures and no prior knowledge of any details of either the surface or bulk line shapes beyond those already mentioned were necessary.

With the plausibility of our approach established, we now analyze the data more critically using a nonlinear least-squares procedure. The only constraints we impose are that there are two components in the data with the same DS line shape. Also, for simplicity we assume that the instrumental response function is purely Gaussian and thus can be easily combined with the Gaussian phonon broadening. (These constraints will be subjected to more careful scrutiny below). All other parameter are variable, and these include the bulk binding energy E_B^b, the total FWHM Gaussian width Γ_G [which includes the Gaussian phonon and spectrometer widths, $\Gamma_G=(\Gamma_{\rm ph}^2+\Gamma_{\rm sp}^2)^{1/2}$], the FWHM Lorentzian lifetime width Γ, the singularity index α, the surface binding energy E_B^s, and its intensity with respect to that of the bulk R_θ. The results of the fits are shown as solid lines in Fig. 3, with the components shown as dashed lines. The surface component is shaded. Numerical values are summarized in Table I.

While the fits in Fig. 3 are excellent, this is itself not definitive support for the validity of our approach since it might be argued that such high-quality fits are to be expected simply because of the large number of free parameters. Justification is obtained from the excellent consistency of the parameters determined from the four independent data sets. The mean Au $4f_{7/2}$ lifetime width is 0.317 ± 0.011 eV, where the uncertainty here represents the standard deviation from the mean. The standard devia-

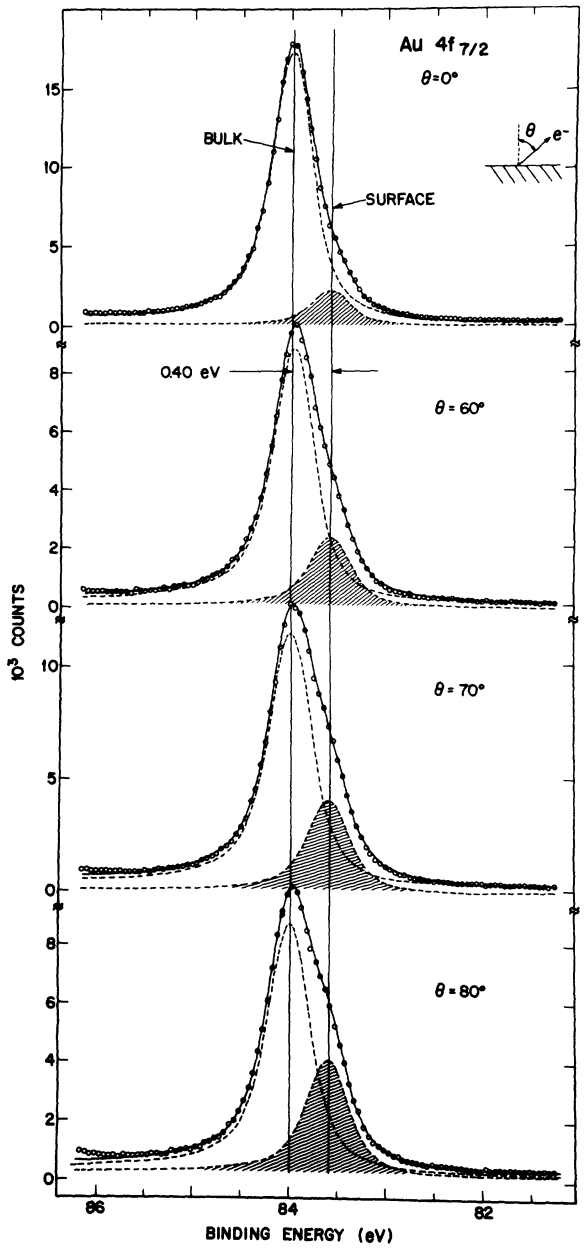

FIG. 3. Least-squares fits to Au $4f_{7/2}$ photoemission data as a function of θ. Each spectrum was fitted *individually* assuming two lines of equal shape with all lineshape parameters and line positions freely adjustable. The surface component is shaded. Note excellent consistency in binding energy of the bulk and surface components for each data set.

tions of the individual values determined from the fits (see Table I) are comparable to this uncertainty, thereby confirming that the high precision of the individual results is indicative of their overall accuracy as well. Including possible sources of systematic error which could effect reproducibility we quote $\Gamma = 0.32 \pm 0.02$ eV.

The mean asymmetry parameter from the fits is 0.052 ± 0.003; we quote 0.052 ± 0.006. This value is somewhat larger than that determined in an earlier study[21] in which the surface-atom contribution was not resolved. This resulted in a slightly larger lifetime width than that reported here.

The Gaussian broadening of 0.296 ± 0.022 eV is an arithmetic average of values showing a monotonic variation with takeoff angle. We quote a value of 0.30 ± 0.05 eV which includes our estimates of reproducibility. While the trend of increasing Γ_G with increasing θ might suggest that the surface-phonon broadening is somewhat larger than the bulk, we note that there is also a corresponding decrease in Γ. Simultaneous least-squares fits of the four data sets with Γ constrained to have the same value for all data sets, described below in our analysis of Ag, show that the absolute value of Γ_G is actually smaller and that the variation of Γ_G with θ is more random than that shown in Table I. Since interpretation of such small variations must rely upon an extremely detailed knowledge of the angular dependence of the spectrometer response function, it is unwise to speculate here on the evidence for surface-phonon broadening in Au. Significantly higher energy resolution is required to address this question satisfactorily. Our conclusions regarding all the other parameters in the fits are, however, rather insensitive to this point.

The bulk- and surface-atom binding energies in the four different data sets allow us to examine the validity of our initial hypothesis that there are only two components in the data. Absolute binding energies are typically known to only $\sim \pm 0.1$ eV, so we assign the bulk Au $4f_{7/2}$ binding energy at $\theta = 0°$ to be 84.000 eV. This value provides a fixed reference point from which the smaller fluctuations in E_B^b between other spectra can be assessed. The corresponding bulk binding-energy values in the 60°, 70°, and 80° spectra are listed in Table I. If there were a third "subsurface" component (between the surface and the bulk layers), then E_B^b would systematically change with θ. That the fluctuations in E_B^b are small and nonsystematic, i.e., that the relative E_B^b values are all within the standard deviations of each other, is direct evidence that such a third component is not present in the data. The second piece of evidence that there are only two components comes from the value of the surface-atom electron binding-energy shift, defined with respect to the bulk value E_B^b in each corresponding spectrum, i.e., not with respect to the assigned reference value. The *surface-atom core-level shift*, $\Delta_{s,b} \equiv E_B^s - E_B^b$, is listed in Table I and is seen to be unusually constant.

TABLE I. Results of *individual* two-line least-squares fits to Au $4f_{7/2}$ data.

Takeoff angle θ	Hole-state lifetime Γ (eV)	Singularity index α	Gaussiaan broadening Γ_G (eV)	Bulk electron binding energy E_B^b (eV)	Surface-bulk shift $\Delta_{s,b}$ (eV)	Surface/(surface plus bulk) intensity ratio f_θ
0°	0.329±0.009	0.048±0.002	0.269±0.022	84.000[a]	−0.401±0.007	0.115±0.005
60°	0.323±0.011	0.054±0.002	0.288±0.019	84.025±0.015	−0.393±0.004	0.215±0.004
70°	0.312±0.010	0.053±0.002	0.311±0.013	84.010±0.014	−0.398±0.003	0.267±0.005
80°	0.305±0.010	0.054±0.002	0.317±0.014	84.014±0.016	−0.399±0.003	0.313±0.003
Average value	0.317±0.011	0.052±0.003	0.296±0.022	84.012±0.010	−0.398±0.003	
Quoted[b] value	0.32±0.02	0.052±0.006	0.30±0.05		− 0.40±0.02	

[a]Assigned value.
[b]Error limits include estimates of reproducibility.

The mean value from the fits is −0.398±0.003 eV; we quote −0.40±0.02 eV. Both the randomness of E_B^b and the constancy of $\Delta_{s,b}$ comprise the necessary and sufficient proof that there are indeed only two components in the data whose line shapes are indistinguishable within the quoted experimental uncertainties.

The final spectral feature that needs to be characterized is the intensity (or, equivalently, area) of the surface-atom component relative to that of the bulk. Knowledge of this allows us to determine the effective thickness D of the surface layer. Values of the surface-to-bulk intensity ratio R_θ determined from the least-squares fits are given in the last column of Table I. With the assumption of an ideally smooth surface, the fractional surface signal $f_\theta = R_\theta/(R_\theta+1)$ is given by the usual expression

$$f_\theta = 1 - e^{-D/\lambda\cos\theta}, \tag{1}$$

where λ is the mean electron escape depth. The minimum D is the effective interlayer spacing for polycrystalline Au. For our purposes here we simply take this value to be the average of the d spacings of the most stable surfaces in an fcc crystal, namely the {111} and {100} surfaces (our conclusions here are insensitive to D). We thus obtain $D = d_{\text{poly}} = \frac{1}{2}(d_{\{111\}} + d_{\{100\}}) = \frac{1}{2}(2.355 + 2.039)$ Å

TABLE II. Determination of escape depth [using Eq. (1)] for 1.4-keV electrons in polycrystalline Au. All values. in Å.

θ_{nom}[a]	λ_{nom}[b]	$\mp f_\theta$[c]	$\pm\theta$[d]	$\pm d_{\text{poly}}$[e]	λ_{avg}[f]
0°	18.0	$^{+0.9}_{-0.8}$	±0.01	±1.3	18.1±2.2
60°	18.2	±0.4	$^{+1.2}_{-1.0}$	±1.3	18.4±2.8
70°	20.7	±0.3	$^{+2.2}_{-1.8}$	±1.5	21.1±3.8
80°	33.8	±0.4	$^{+8.4}_{-5.6}$	±2.5	35.8±9.9

[a]Nominal experimental takeoff angle (refraction effects not included).
[b]Nominal escape depth assuming no uncertainty in f_θ, θ, and d_{poly}.
[c]Uncertainty in λ_{nom} due solely to uncertainty of fractional surface intensity f_θ as determined from least-squares fits, see Table I (note opposite sign dependence of λ_{nom} and f_θ uncertainties).
[d]Uncertainty in λ_{nom} due solely to uncertainty in nominal experimental takeoff angle θ_{nom}.
[e]Uncertainty in λ_{nom} due solely to uncertainty in average surface-atom d spacing for polycrystalline Au (see text).
[f]Average escape depth of upper- and lower-limit values determined from *correlated* uncertainties in f_θ, θ, and d_{poly} (refraction effects not included).

$=2.20\pm0.16$ Å. The mean electron escape depths are solved for at the various angles and the results are given in Table II. We have listed the individual uncertainty contributions to λ arising from f_θ (from Table I), $\theta(\pm2°)$, and d_{poly} assuming that each acts independently of the others. The last column represents a more realistic average λ since it incorporates all the uncertainties of the aforementioned parameters assuming they are correlated. From Table II we see a monotonically increasing trend of λ_{avg} with increasing θ coupled with a corresponding trend in its uncertainty. The major source of this latter trend is due to the uncertainty in θ. The value of λ_{avg} for $\theta=80°$ is undoubtedly in error because of surface-roughness effects, i.e., a breakdown in our initial assumption of an ideally smooth surface. Another source of error is our neglect of electron refraction at the surface, which becomes more important as θ_{nom} increases. The external nominal angle is related to the internal angle θ_{in} by

$$\theta_{\text{in}}=\sin^{-1}(\sin\theta_{\text{nom}}[E/(E+eV_0)]^{1/2}) , \tag{2}$$

where E is the electron kinetic energy and V_0 is the inner potential. Assuming $E=1400$ eV and $eV_0=14$ eV, θ_{nom} decreases from 80° (70°) to 78.5° (69.2°), which in turn decreases $\lambda_{80°}$ ($\lambda_{70°}$) from 35.8 Å (21.1 Å) to 29.4 Å (20.0 Å). These effects are sufficiently small to ignore for the purpose of this discussion, which is to establish the qualitative value of λ. We see from Table II that despite the monotonic trend of λ_{avg} with θ, the λ_{avg} values for the $\theta=0°$, 60°, and 70° data fall within the quoted error limits of each other; the mean value of λ_{avg} is 19.2 ± 1.6 Å (we quote 19 ± 3 Å). This is taken as direct evidence of the precision of the independent determinations of λ_{avg}. The accuracy of these values can only be assessed by comparisons with other independent results.[3] Henke's[22] carefully determined value of $\lambda=19$ Å for 1.4-keV electrons in polycrystalline Au determined by a different method is in excellent agreement with our result, while a still different method for determining λ by Klasson *et al.*[23] gave 26 ± 3 Å. The important conclusion of this agreement is that we have determined the surface-atom component to originate from a layer one atom thick, in agreement with our initial expectations.

The above novel approach for obtaining λ completes the characterization of the surface-atom component in the core-level photoemission spectrum. We now know its line shape, its binding energy with respect to the bulk, and the thickness of the layer which gives the unique surface signal. It must be true that the existence of the surface-atom core-level component is related to the surface density of states (see Sec. III), and comparable information about them is clearly desirable. In the absence of corresponding criteria to determine independently the weighting coefficients for the two valence-band spectra measured at two different takeoff angles (the surface and bulk DOS shapes and intensities depend upon details of the band structure and the partial photoabsorption cross sections), it would still be possible to take difference spectra with ratios determined by the escape depths appropriate for the material and θ. The obvious shortcoming of this approach is that such information is rarely known to the accuracy required and, moreover, possible surface-roughness effects at grazing emission angles could (as we have already seen) preclude the applicability of independently determined escape depths. The alternate approach is to use the same weighting coefficients which separate the *core*-level spectra in bulk and surface components and apply them to the *valence*-band spectra taken at the same angles.

There are a number of points to be made about this approach.

(a) It is equivalent to using empirical electron escape depths for the conduction electrons since the kinetic energy of the Au $4f$ electrons (1.40 keV) photoexcited with Al $K\alpha$ radiation is essentially the same as that of the conduction electrons (1.48 keV).

(b) It has the advantage of removing any angular-dependent instrumental effects since these will be the same for both the core and valence spectra taken with the same instrument.

(c) Its application should be generally valid for polycrystalline materials and for high kinetic energy photoelectrons since the respective effects of azimuthal angular variations in the valence transition probabilities[24] and of refraction at the surface are unimportant.

(d) It is purely empirical and involves *no* further adjustable parameters, i.e., the valence surface-bulk separation is uniquely determined once the core surface-bulk separation is obtained.

Now there are actually two different methods of applying this procedure. The first involves the weighting coefficients β and γ used above to separate the core-level spectra. These are multiplied and divided by the appropriate counting-rate factors according to

$$\begin{aligned} &\gamma_{\text{VB}}=\gamma T , \\ &\beta_{\text{VB}}=\beta/T , \\ &T=\left[\frac{t_C}{t_{\text{VB}}}\right]_{70°}\left[\frac{t_{\text{VB}}}{t_C}\right]_{0°} . \end{aligned} \tag{3}$$

Here t_C and t_{VB} are the total counting times of the core and valence-band spectra, respectively. [The ratio $(t_{\text{VB}})_{0°}/(t_{\text{VB}})_{70°}$ accounts for the difference in

total accumulated counts between the $\theta=0°$ and 70° valence-band data while the ratio $(t_C)_{70°}/(t_C)_{0°}$ corrects for the constant difference in instrumental collection efficiencies at the different angles.] The only requirement for this method is that the incident x-ray flux must remain constant during the course of the measurements, a condition that was tested for and fulfilled in these experiments. The core-level weighting coefficients β and γ could be either determined empirically as in Fig. 2 or computed from the results of the least-squares procedure. Using the latter values, we replace the empirically determined β and γ coefficients in Eq. (3) by

$$\beta_{\mathrm{lsq}}=\frac{a^C_{\mathrm{lsq},0°}}{a^C_{\mathrm{lsq},70°}}=A^C_{\mathrm{lsq}}\ ,$$
$$\gamma_{\mathrm{lsq}}=\frac{R_{0°}}{R_{70°}}A^C_{\mathrm{lsq}}\ , \tag{4}$$

where $a^C_{\mathrm{lsq},\theta}$ is the least-squares computed area of the bulk core-level component and R_θ $[=f_\theta/(1-f_\theta)]$ is the computed surface-to-bulk intensities ratio (areas) in the θ spectrum. We have compared our empirically determined β value with β_{lsq} for the $\theta=0°$ and 70° data and found them to agree to better than 1%. This is not surprising since we saw (Fig. 2) that β is very sensitive to small contributions of bulk intensity on the high-binding-energy side of the surface component. The values of γ and γ_{lsq}, on the other hand, agreed to within only 6%. The least-squares result is probably more reliable since we saw (Fig. 2) that the low-binding-energy side of the bulk component is not very sensitive to small contributions from the surface.

The second method of applying the surface-bulk DOS separation using core-level data overcomes one shortcoming of using Eq. (3), namely that the coefficients γ_{VB} and β_{VB} are not unique because they contain relative intensity information (i.e., counting times t) not inherent to the general surface-bulk DOS decomposition procedure. This can be avoided by using the fractional surface coefficients f_θ determined from the least-squares fits according to

$$\gamma'_{\mathrm{VB}}=\frac{f_{0°}}{f_{70°}}A_{\mathrm{VB}}\ ,$$
$$\beta'_{\mathrm{VB}}=\frac{(1-f_{70°})}{(1-f_{0°})}\frac{1}{A_{\mathrm{VB}}}\ , \tag{5}$$
$$A_{\mathrm{VB}}=\frac{a^{\mathrm{VB}}_{70°}}{a^{\mathrm{VB}}_{0°}}\ ,$$

where a^{VB}_θ is the total empirical area of the valence-band spectrum at a given θ. Now the ratios of the fractional surface and bulk coeffcients represent a more fundamental description of the separation procedure since two valence-band spectra whose areas have been normalized have prescribed fractions of surface and bulk intensity independent of details of the instrumental collection efficiency. [Parenthetically, the same description could be given for the core-level data by replacing γ'_{VB}, β'_{VB}, and A_{VB} in Eq. (5) with γ'_C, β'_C, and $A_C=a^C_{70°}/a^C_{0°}$, where now a^C_θ is the total empirical area of the core-level spectrum.]

In the upper portion of Fig. 4 we show the raw valence-band spectra measured at $\theta=0°$ and 70°. Either Eq. (3) or (5) may be used to determine the appropriate weighting coefficients, and for completeness we give the results for both. The f_θ values in Table II are used to predict that for hyothetically area-normalized valence-band spectra γ'_{VB} would be 0.43 ± 0.02 and β'_{VB} would be 0.83 ± 0.01. Since the integrated areas of the real 0° and 70° data are in the ratio of 2.0:1 (note the different left- and right-hand scale assignments in Fig. 4), these values must be modified according to Eq. (5) to give

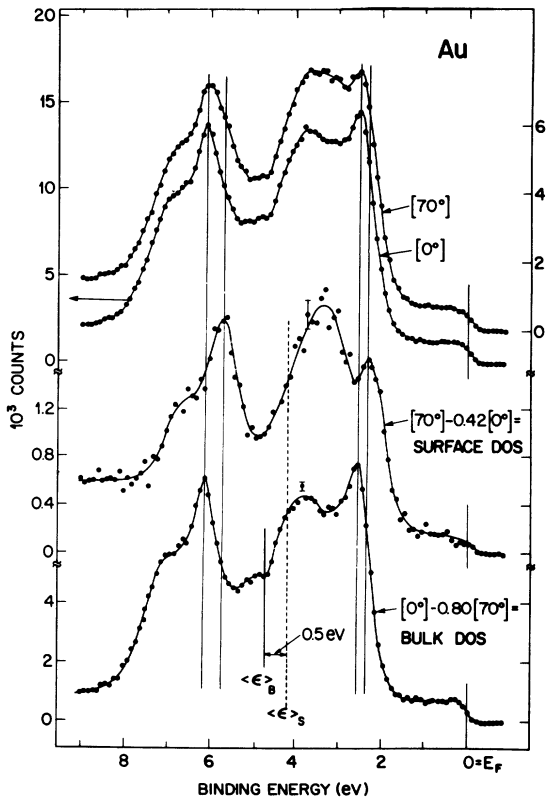

FIG. 4. Separation of Au bulk and surface density of states from the difference between $\theta=0°$ and 70° spectra. Note different scales for raw data. Weighting factors 0.42 and 0.80 were determined from corresponding *core*-level spectra as in Fig. 2. Centers of gravity $\langle\epsilon\rangle$ for bulk and surface DOS are also shown.

$\gamma'_{VB}=0.86\pm0.04$ and $\beta'_{VB}=0.41\pm0.01$. Using Eq. (3) and the empirical values of γ and β, we independently obtained $\gamma_{VB}=0.81\pm0.08$ and $\beta_{VB}=0.41\pm0.02$. (This agreement is simply a restatement of that previously mentioned between γ and γ_{lsq} between β and β_{lsq}). Since the results for the bulk DOS are insensitive to γ_{VB} vs γ'_{VB} we used the former, and these are shown in the lower portion of Fig. 4. For comparison the surface DOS is shown above it. Note that because a larger fraction of data is subtracted in the separation of the surface DOS relative to the bulk DOS ($\sim$80% versus 40%), the statistics for the former are poorer. Nevertheless, the differences between the two valence-band spectra are readily apparent. The details of these differences are discussed in Ref. 14 where it will be seen that two spectral properties of the bulk and surface DOS, namely their widths and their centers of gravity, contain important information regarding the understanding of the SCS. We conclude our discussion of Au with the determination of these two quantities. Only the d part of the valence band will be considered.

The center of gravity $\langle\epsilon\rangle$ of the valence d band is described by I_1/I_0, where I_0 and I_1 are the zeroth and first moments. The integrations are performed between upper and lower limits which define the total d-band width. For Au these are taken to be approximately 8.5 and 1.5 eV, respectively. Also, the integrations are performed on background-subtracted data since only the elastically scattered electrons are of interest. The subtraction algorithm used is based on the assumption that the inelastic intensity at each kinetic energy is proportional to the integrated no-loss area at higher energies. (Our results are insensitive to the details of the subtraction procedure because the background is so small.) The width W of the valence d band can be shown to be described by $I_2/I_0-(I_1/I_0)^2$, where I_2 is the second moment. It, too, is determined from the background-subtracted data taken over the same upper and lower limits as for $\langle\epsilon\rangle$. To place error bars on $\langle\epsilon\rangle$ and W we have varied both the background and the coefficients γ_{VB} and β_{VB} within the conservative limits of $\pm5\%$ of their respective values. From this procedure we find that the surface DOS width is $(8\pm2)\%$ narrower than that of the bulk and that the center of gravity shift between the surface and the bulk DOS, $\langle\epsilon\rangle_s-\langle\epsilon\rangle_b$, is -0.5 ± 0.1 eV.

B. Silver

Inspection of the data shown in Fig. 1 makes it apparent that $\Delta_{s,b}$ for Ag is much smaller than that for Au. Although the Ag $3d_{5/2}$ line is inherently narrower than the Au $4f_{7/2}$ line, only a slight deviation on the low-binding-energy side is discernible with increasing takeoff angle. Without knowledge of the SCS in Au, this low-binding-energy intensity might easily be ignored or explained away as arising from angular-dependent instrumental broadening. Even with knowledge of the SCS in Au and a suspicion of similar behavior in Ag, it is not possible to analyze Ag data using the procedures described for Au because the two Ag photopeaks (surface and bulk) are separated by less than half their width. In particular, linear combinations of raw data sets gave

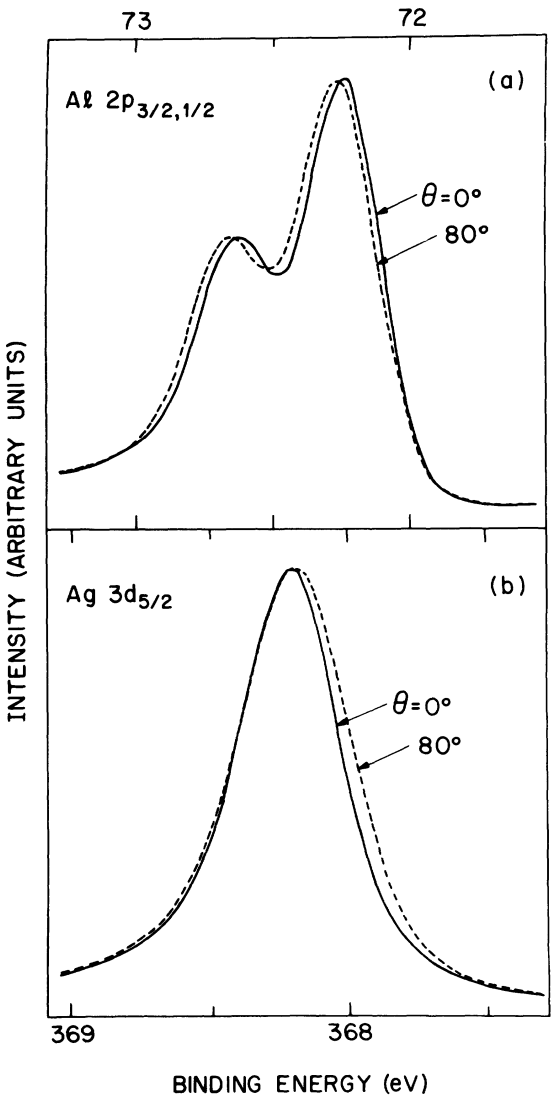

FIG. 5. Results of least-squares fits to Al $2p_{3/2,1/2}$ and Ag $3d_{5/2}$ data at $\theta=0°$ and 80°. Data were individually fitted assuming only one bulk component. Compare small symmetric shift to higher binding energy for $\theta=80°$ Al $2p$ data with the small asymmetric shift to lower binding energy for $\theta=80°$ Ag $3d_{5/2}$ data.

TABLE III. Results of one-line least-squares fits to Al $2p$ data.

Takeoff angle θ	Hole-state lifetime Γ (eV)	Singularity index α	Gaussian broadening Γ_G (eV)	Bulk electron binding energy E_B^b (eV)	Spin-orbit splitting Δ	$2p_{3/2}/2p_{1/2}$ intensity ratio R
0°	0.052±0.009	0.121±0.004	0.266±0.007	72.500[a]	0.402±0.002	1.976±0.028
80°	0.051±0.010	0.114±0.003	0.280±0.007	72.518±0.010	0.405±0.002	1.992±0.032
Quoted[b] value	0.05±0.02	0.12±0.01	0.27±0.02		0.40±0.01	1.98±0.04

[a]Assigned value.
[b]Error limits include estimates of reproducibility.

ill-defined line shapes, and fully unconstrained least-squares fits using two components gave nonunique and unphysical results due to parameter correlations. Lacking direct evidence of surface-atom photoemission in Ag, then, we must first demonstrate the existence of a SCS in Ag and then develop procedures to extract the surface-atom contribution. We now examine how this is done.

The first problem is that it is difficult to distinguish the difference between a single instrumentally broadened peak and two unresolved peaks. To check for angle-dependent instrumental broadening we have least-squares analyzed normal and grazing photoemission spectra from the very narrow Al $2p$ core levels assuming the data to be composed of a single bulk spin-orbit doublet. The results of the fits are shown in Fig. 5(a) and the numerical values are given in Table III. There is excellent consistencey between the line shapes of the two different data sets, with only a small and nearly *symmetric* shift to higher binding energy at grazing emission angle. We attach no physical significance to this shift in view of the very small (-0.057 ± 0.007 eV) shift of opposite sign measured by Chiang and Eastman[25] and the fact that this shift is comparable to the fluctuations in E_B^b for Au. There is also a finite but small increase in Γ_G with increasing θ. The Ag $3d_{5/2}$ data taken at various emission angles have been similarly least-squares analyzed with a single component. The numerical results are summarized in Table IV and the fits at $\theta=0°$ and 80° are shown in Fig. 5(b). In contrast to the Al $2p$ data, there is a small and *asymmetric* shift to lower binding energy at grazing emission angle. More importantly, there is a systematically increasing Gaussian broadening, which is outside the uncertainty and reproducibility limits of the Gaussian contribution determined from the narrower Al $2p$ data. This behavior in Ag is therefore not an artifact of instrumental broadening but is, instead, consistent with the presence of a surface component at smaller binding energy, just as in the case of Au.

Since the overall shape (i.e., singularity index and lifetime width) of the single-line fits to the Ag $3d$ line does not vary appreciably with takeoff angle, the monotonically varying shift in binding energy can be taken as a measure of the centroid shift due to the increasing strength of the surface component. In order to test whether the results are compatible with this supposition we use the following model. We assume that the data contain two components at fixed energies with the same shape, as in the case of

TABLE IV. Results of one-line least-squares fits to Ag $3d_{5/2}$ data.

Takeoff angle θ	Hole-state lifetime Γ (eV)	Singularity index α	Gaussian broadening Γ_G (eV)	Bulk electron binding energy E_B^b[a] (eV)
0°	0.281±0.002	0.059±0.001	0.238±0.005	368.192[b]
60°	0.277±0.002	0.063±0.002	0.271±0.005	368.179±0.010
70°	0.270±0.003	0.067±0.001	0.290±0.006	368.172±0.010
80°	0.269±0.002	0.068±0.001	0.297±0.004	368.168±0.010

[a]Here $\Delta_{s,b}\equiv0$ and, from Eq. (7), $\bar{E}\equiv E_B^b$.
[b]From extrapolated value assigned at 368.200 eV, see text.

Au, with the fractional intensity of the surface component given by Eq. (1). The energy of the centroid, $\bar{E}$, is then

$$\bar{E}=(1-f_\theta)E_B^b+f_\theta E_B^s$$
$$=E_B^b+f_\theta\Delta_{s,b}\ . \quad (6)$$

If $D\ll\lambda\cos\theta$,

$$\bar{E}\approx E_B^b+\Delta_{s,b}D/\lambda\cos\theta\ . \quad (7)$$

By plotting $\bar{E}$ vs $1/\cos\theta$ we should obtain a straight line in the region where the above equation is satisfied. Note that this approach is valid so long as $\Delta_{s,b}$ is small with respect to the linewidth of each component.

The results of the single-line fits for Ag $3d_{5/2}$ using Eq. (7) are given in Table IV and the values for $\bar{E}$ are plotted in Fig. 6. [Because the condition $D\ll\lambda\cos\theta$ is less well satisfied for $\theta=80°$ and because of surface-roughness considerations (see analysis for Au), we have not included the $\theta=80°$ data in our analysis.] The fact that the three data sets do approximate a straight line and have a scatter compatible with the reproducibility of each measurement indicates that the model provides a good representation of the physical situation. According to Eq. (7) the intercept at $1/\cos\theta=0$ yields the binding energy of the bulk components. (The extrapolation into the region where $1/\cos\theta$ is less than 1 can be readily justified.) The slope gives the quotient of the surface-bulk shift and the escape depth defined in units of the atomic layer thickness D. The extrapolated bulk binding energy corresponds to channel 50.22, which we assign to be 368.200 eV. Using an independently measured value of $\lambda=21$ Å (Ref. 26) we obtain an estimate for $\Delta_{s,b}=-0.12$ eV. A calculated value of $\lambda=14$ Å (Ref. 27) yields $\Delta_{s,b}=-0.08$ Å.

With the bulk binding energy E_B^b evaluated it would now be feasible to perform two-line fits to the individual data sets to determine the other spectral parameters. However, since the lifetime width Γ of the Ag $3d$ hole state and the singularity index α have

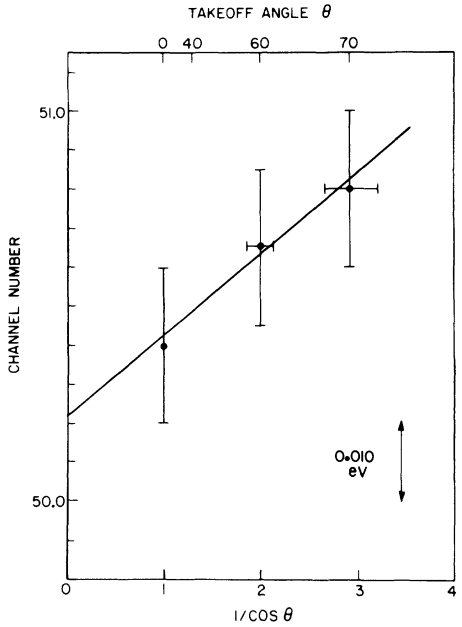

FIG. 6. Demonstration of surface-atom photoemission in Ag $3d_{5/2}$ spectra. Binding energies in channel number (one channel equals 0.050 eV) are determined from one-line least-squares fits of Ag $3d_{5/2}$ data at $\theta=0°$, 60°, and 70°. Monotonic variation with θ is described by Eq. (7).

values which should be the same in all data sets it is advantageous to make a *simultaneous* fit to all the data in which these additional parameters automatically have a common but adjustable value. Other parameters may also be constrained to have either common or fixed common values.

As a test of this formalism the Au spectra were fitted leaving all parameters freely adjustable, but with common values for $\Delta_{s,b}$ Γ, α, and E_B^b. The results, see Table V, differ slightly from those obtained above in Table I because E_B^b is constrained to be the same for all spectra, but there is no disagreement outside of the quoted uncertainties. The values of Γ_G for the four data sets increase at the

TABLE V. Results of *simultaneous* least squares fits to data at all takeoff angles. All quoted error limits include estimates of reproducibility.

	Hole-state lifetime Γ (eV)	Singularity index α	Gaussian broadening Γ_G (eV)	Surface-bulk shift $\Delta_{s,b}$ (eV)
Au $4f_{7/2}$	0.339±0.02	0.048±0.006	0.276±0.03[a]	−0.389±0.01
Ag $3d_{5/2}$	0.274±0.01	0.066±0.006	0.262±0.03[a]	−0.076±0.03
Cu $2p_{3/2}$	0.595±0.01	0.042±0.006	[0.230][b]	−0.241±0.02

[a]Average of angle-dependent values.
[b]Constrained.

larger takeoff angles, viz., 0.266, 0.258, 0.293, and 0.286 eV for $\theta=0$, 60°, 70°, and 80°, respectively, but the variation is much weaker than that obtained from the individual fits, see Table I. The present results are probably more reliable because the lifetime widths from the individual fits had a nonphysical decrease with takeoff angle whch was largely responsible for the increase in Γ_G. The reason this simultaneous least-squares method was not used in the primary analysis of the Au data is that the ability to obtain *independent and consistent* values for $\Delta_{s,b}$ from the four spectra provided an important confirmation of the validity of the SCS concept and our fitting procedures.

An attempt to apply this simultaneous least-squares procedure to the Ag spectra with all the parameters free was less successful in determining unambiguous values for all the parameters. (The resulting f_θ values lacked statistical significance because there is insufficient information in the line shape to distinguish the bulk and surface components.) By imposing an additional constraint, e.g., by forcing all the bulk components to lie at the same *fixed* energy (namely, the channel number determined from the extrapolation in Fig. 6), meaningful results are readily obtained with all other parameters freely adjustable, see Table V. The value of -0.076 eV for $\Delta_{s,b}$ obtained from this procedure can be combined with the slope from Fig. 6 to given an independent estimate of the escape depth in Ag at 1100 eV, yielding a value of 13 Å. The uncertainty in this value is estimated to be $\pm 50\%$. We quote a value for $\Delta_{s,b}$ in Ag to be -0.08 ± 0.03 eV. It must be recognized that satisfactory fits can also be obtained from a comparatively wide range (± 0.01 eV) of bulk-atom binding energies. However, these other fits differ largely in the intensity assigned to the surface component and, significantly, to a much lesser extent in $\Delta_{s,b}$. These facts have been taken into account in the quoted uncertainties of the escape depth and $\Delta_{s,b}$ for Ag. The fits obtained with E_B^b constrained to 368.2 eV and $\Delta_{s,b}$ constrained to -0.08 eV are shown in Fig. 7.

The many-body singularity index $\alpha=0.066\pm0.003$ is in agreement with other determinations,[28,29] and corresponds closely to a theoretical evaluation.[29] Γ_G again exhibits a variation with θ, viz., 0.233, 0.260, 0.274, and 0.280 eV for $\theta=0°$, 60°, 70°, and 80°, but unlike the case of Au this variation is not random. While these results suggest extra phonon broadening in the surface signal it is clearly not possible to confirm this with the present data. The question of surface-phonon broadening should be pursued in cases where the two components are more clearly resolved so that an analysis without constraints can be carried out.

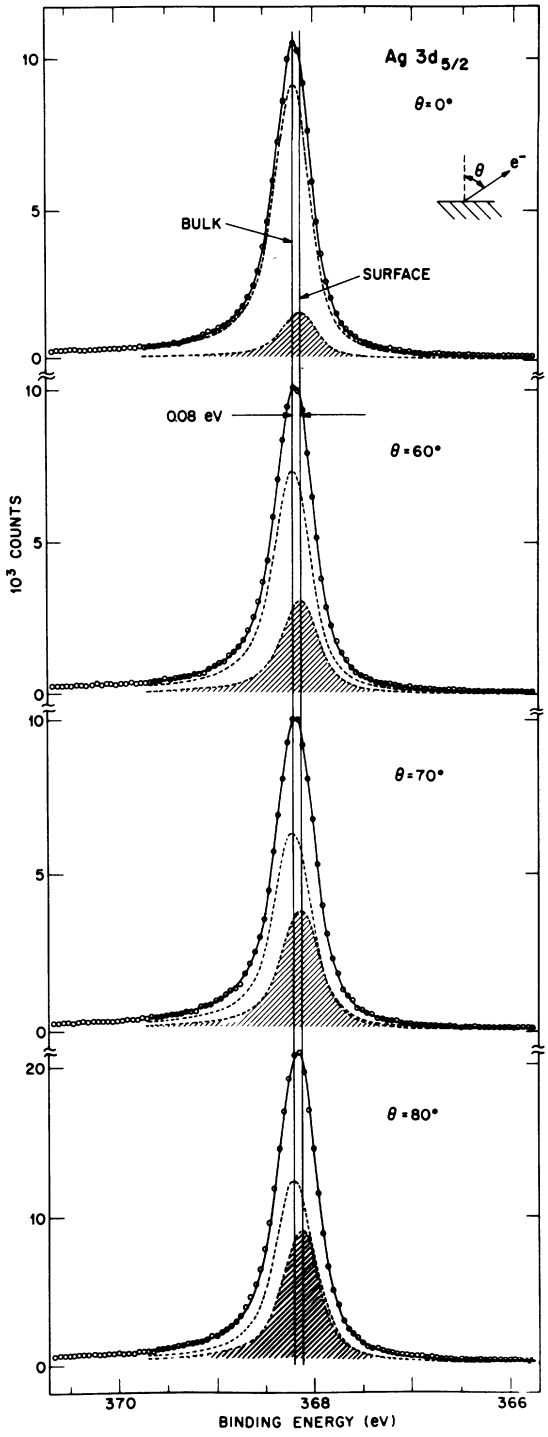

FIG. 7. Least-squares fits to Ag $3d_{5/2}$ data as a function of θ. All data sets were fitted *simultaneously* with lifetime broadening, singularity index, and surface binding energy having freely adjustable but common values. The bulk binding energy was constrained to a value determined from extrapolation in Fig. 6.

C. Copper

Inspection of Fig. 1 shows that the case of Cu is in many ways comparable to that of Ag. The SCS is closer to that of Au than of Ag, but the Cu $2p_{3/2}$ core-level width is also much larger than that of the Ag $3d_{5/2}$ level. The ratio of shift to linewidth is, however, slightly more favorable than in Ag. An attempt to follow the single-line-shift method used for Ag, i.e., Eq. (6), failed because single-line fits gave systematic variations in line shape (specifically α) with takeoff angle. The fits were also relatively poor in the high-energy tails. This itself is already a clear indication that there is more than one component in the spectra.

In Fig. 8 we compare a one-line and a two-line fit to the Cu $2p_{3/2}$ data taken at 75° takeoff angle. The difference in quality of fit is best assessed by the residuals shown in the lower half of the figure. If the noise in the data were entirely due to counting statistics the residuals would fluctuate randomly about zero when an adequate fit is obtained. The one-line fit shows systematic trends in the residuals indicating that one line is not able to represent the data satisfactorily. In the two-line fit the ideal of randomness is approached much more closely. The ratio of the sum of the squares of the deviation to the total number of counts provides a simple index of the quality of fit. The one-line fit gives 1.18, the two-line fit 0.630. An attempt to make independent two-line fits to all the data sets, as was done in the case of Au, did not lead to satisfactory results, largely because $\Delta_{s,b}$ was not well determined from the low-angle data.

We have consequently made *simultaneous* fits to the Cu spectra. The major advantage of the simultaneous least-squares method lies in the fact that those parameters which are inherently identical can be constrained to be the same in the four spectra but at the time remain adjustable by least squares. This gives confidence that the other parameters are not compromised. With all parameters free these fits gave an unphysically small value for Γ_G. With Γ_G constrained to 0.23 eV, the lower limit set by the instrumental response function, the procedure converged rapidly to the values shown in Table V. The fits are shown in Fig. 9. In this case there is sufficient information in the data so that the position of the bulk component could be independently determined for each data set. The resulting values of E_B^b are consistent and show only small random fluctuations, i.e., 932.700 (assigned), 932.713, 932.734, and 932.722 eV for $\theta=0°$, 30°, 60°, and 75°, respectively. The quoted value for the lifetime width is 0.60 ± 0.02 eV and the many-body singularity index has a value of 0.042 ± 0.006, testifying to the non-free-electron-like character of the conducting electrons.[28] $\Delta_{s,b}$ has a quoted value of -0.24 ± 0.02 eV, intermediate between those of Au and Ag. The least-squares procedure also yields satisfactory intensities for the sur-

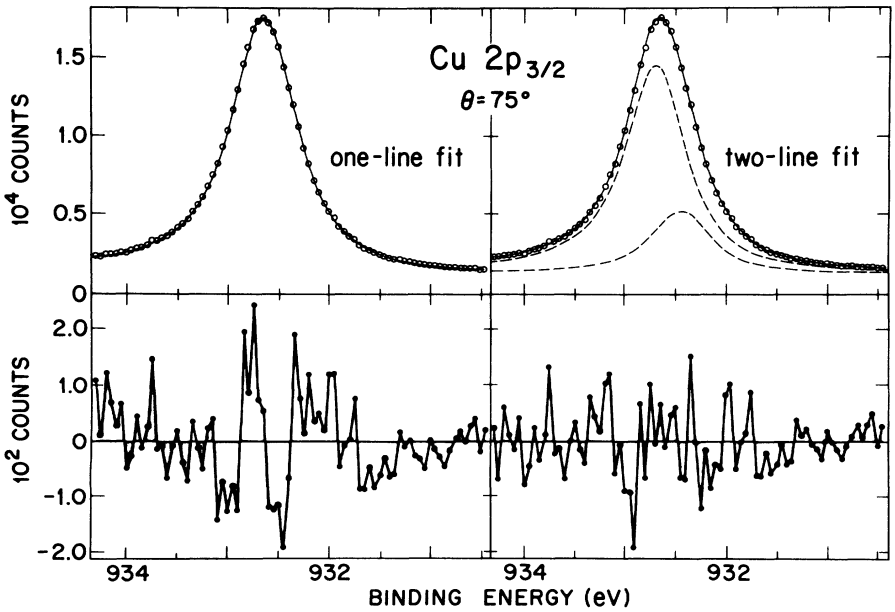

FIG. 8. Demonstration of surface-atom photoemission in Cu $2p_{3/2}$ data. Residuals for least-squares fit using one line show nonrandom fluctuations whereas those using two lines (surface and bulk) are random and more representative of data.

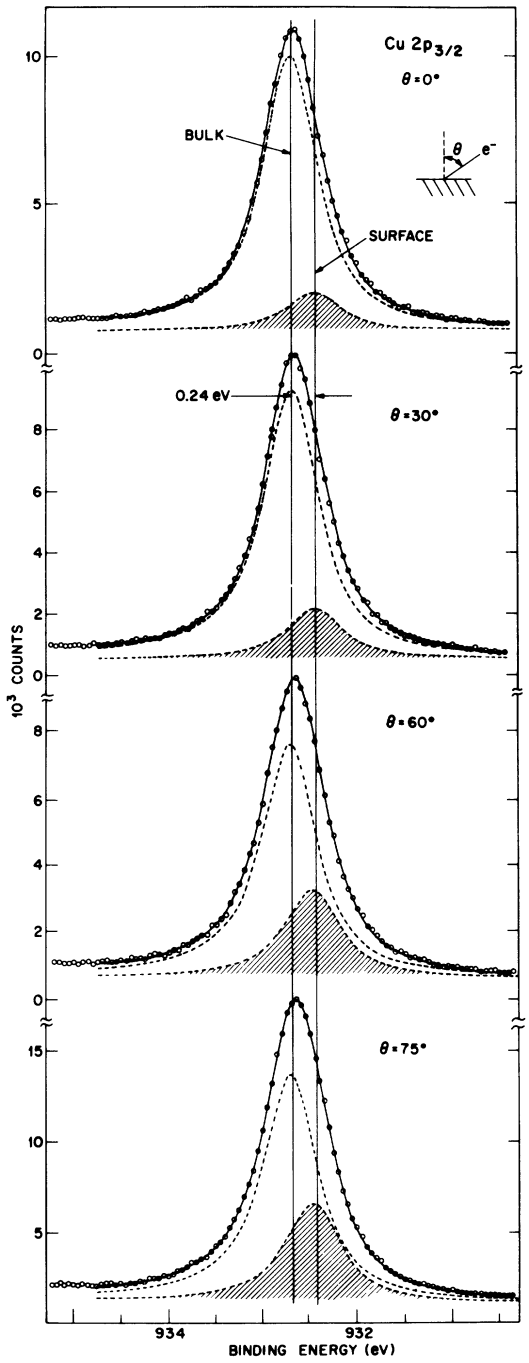

FIG. 9. Least-square fits to Cu $2p_{3/2}$ data as a function of θ. All data sets were fitted *simultaneously* with lifetime broadening, singularity index, and surface binding energy having freely adjustable but common values. The Gaussian broadening was constrained to lower limit set by instrumental response function.

face components, i.e., 0.120±0.017, 0.158±0.019, 0.272±0.030, and 0.307±0.025 for θ=0°, 30°, 60°, and 75°. Using the procedure described for the case of Au these intensities correspond to respective electron escape depths λ_{avg} (with quoted correlated uncertainties) of 15.6±3.1, 13.4±2.7, 12.7±2.9, and 21.8±6.5 Å. The mean of the 0°, 30°, and 60° values is 13.9±1.5 Å (we quote 14±3 Å), in good agreement with experimental[3] and theoretical[26] values.

III. SUMMARY

The analysis presented above has established the nature of the change in the electronic structure at the surface of evaporated noble metals and its effect on core-electron binding energies. Although this information is obtained from photoemission, a final-state spectroscopy, our conclusions pertain largely to the initial state. This was demonstrated in the case of Au by showing that within experimental error the bulk and surface atoms have the same line shape and therefore the same final-state screening response. The individual surface and bulk responses were isolated using a linear combination of spectra, a technique which does not require any assumptions about the line shape. Our conclusions were put on a quantitative basis by least-squares fitting the Doniach-Šunjić line shape to the data. Both analyses show that the data are well represented by only two components, bulk and surface. The intensity of the surface signal and its change with takeoff angle show that the surface component comes from the first atomic layer. The second atomic layer is experimentally indistinguishable from the bulk. These facts allow a direct determination of the electron escape depth in terms of the metal d spacing without the well-known problems associated with overlayer experiments. For Au this value is measured to be 19±3 Å at 1400 eV kinetic energy, in very good agreement with independent estimates. The other major result of this study is the determination of the surface-atom core-electron binding-energy shift, which arises from the band narrowing at the surface and the attendant charge redistribution. The connection between the valence- and core-electron modifications at the surface is discussed in detail in the following paper.[14] For Au the value of the SCS, $\Delta_{s,b}$, is −0.40±0.02 eV, with the sign indicating a lower binding energy for the surface component.

Once the fractional bulk and surface contributions to the total *core*-electron signal are known for two takeoff angles, they can be used to isolate the bulk and surface contributions to the *valence*-band spectrum. The process is again one of linear combination and requires no additional assumptions. It is, in fact, a general procedure which should find its way in future surface-atom studies of core and valence photoemission in other systems. The results obtained here for Au are illuminating, showing not

only the anticipated density-of-states narrowing but also a centroid shift towards E_F which is comparable to the core-electron shift. This part of the analysis directly exhibits the modifications in the surface band structure responsible for the surface core-electron shift.

The Cu core-level data do not contain sufficient information to define the shapes of the bulk and surface components individually. Following the results obtained for Au, the Cu bulk and surface line shapes were assumed to be the same and the assumption tested by fitting two identical lines to the data. The two-line fits to the Cu data were clearly superior to the single-line fits, but the line-shape parameters determined by the fits did not have adequate statistical significance. This problem was overcome by fitting the data for all takeoff angles simultaneously, so that parameters like the lifetime width and surface-atom shift would have common values. A well-defined value of -0.24 ± 0.02 eV for $\Delta_{s,b}$ was then obtained, and the surface-atom intensities again indicated that the surface signal comes from only the first atomic layer. Quantitative evaluation led to an escape depth in Cu of 14 ± 3 Å at 550 eV kinetic energy, also in good agreement with other determinations.

It is worth noting that the ability to determine $\Delta_{s,b}$ for Cu is limited not by the instrumental resolution of $\lesssim 0.24$ eV, but by the $2p_{3/2}$ hole-state lifetime width Γ of 0.6 eV. It is a clear indication of the power of simultaneous least-squares analysis that a component shifted by only 0.4Γ could be established with confidence.

In the case of Ag the individual data sets at different takeoff angles give no indication of the presence of a shifted surface component. They are each well fitted by a single DS line shape. The only clue to the presence of a surface component is found in a small shift in line position and correlated with this, a systematically increasing linewidth with takeoff angle which is outside experimental uncertainties as determined from analysis of narrower Al $2p$ data. The shift information was used to determine the position of the bulk component. With this parameter predetermined and fixed, a simultaneous fit to all the data then yields a reasonably well-defined value of -0.08 ± 0.03 eV for $\Delta_{s,b}$. Using the predetermined value of the bulk binding energy leads to an escape depth of $\sim 13\pm7$ Å, in agreement with a theoretical determination. The relative value of $\Delta_{s,b}$ for Ag is only 0.3Γ and its absolute value is very much smaller than that of Au or Cu. This is understood in terms of the fact that the d band of Ag is less strongly hybridized with the s-p conduction band than are those of Cu or Au, i.e., it is more corelike and less subject to charge redistribution at the surface. This result suggests that metals like Zn, Ga, Cd, In, Hg, and Tl should also have small surface-atom shifts. A detailed discussion of shifts in the noble and transition metals, as well as in the free-electron-like and rare-earth metals, is given in the following paper.[14]

One issue raised by the data analysis, which remains largely unresolved, is the possibility that the surface signal has greater phonon broadening than the bulk. An attempt to include this feature in the simultaneous fits was largely unsuccessful. In the individual fits for the case of Au, the overall phonon width did increase slightly as the surface signal increased, but the scatter was comparable to the effect, forcing us to conclude that we have no convincing evidence for surface-phonon broadening in Au. For the case of Cu no phonon broadening of any kind was detected because of the large Lorentzian lifetime width, which obscures small Gaussian phonon broadening. Only for the case of Ag was there a systematic increase in phonon widths with takeoff angle which merits further consideration. In view of the difficulty of the Ag analysis, however, it seems prudent to consider this an open question in need of further experimental investigation.

In summary, we have shown that the modification of electronic structure at the surface of evaporated noble metals is confined to the first atomic layer, have determined the shift in the core-electron binding energy at the surface, and have shown it to be a predominantly initial-state effect. For Au we have also isolated the surface density of states and shown that it is both narrowed and shifted toward E_F. Finally, we have used the relative intensities of the surface and bulk signals to measure the escape depth in terms of the metallic d spacing. Our analysis procedures and conclusions are quite general and should be applicable for studying both core and valence photoemission from clean surfaces of other systems.

[1]K. Siegbahn, C. Nordling, A. Fahlman, R. Nordberg, K. Hamrin, J. Hedman, G. Johansson, T. Bergmark, S.-E. Karlsson, I. Lindgren, and B. Lindberg, *ESCA—Atomic, Molecular and Solid State Structure Studied by Means of Electron Spectroscopy* (Almqvist and Wiksells, Uppsala, 1967), pp. 139—141.

[2]Y. Baer, P. F. Hedèn, J. Hedman, M. Klasson, and C. Nordling, Solid State Commun. 8, 1479 (1970).

[3]C. J. Powell, Surf. Sci. 44, 29 (1974), and references therein.

[4]J. E. Houston, R. L. Park, and G. E. Laramore, Phys. Rev. Lett. 30, 846 (1973).
[5]C. Webb and P. M. Williams, Phys. Rev. Lett. 33, 824 (1974).
[6]M. Mehta and C. S. Fadley, Phys. Rev. Lett. 39, 1569 (1977).
[7]P. W. Chye, I. Lindau, P. Pianetta, C. M. Garner, and W. Spicer, Phys. Lett. 63A, 387 (1977).
[8]J. C. Fuggle and D. Menzel, Chem. Phys. Lett. 33, 37 (1975).
[9]A. Barrie and A. M. Bradshaw, Phys. Lett. 55A, 306 (1975).
[10]J. C. Fuggle and D. Menzel, Surf. Sci. 53, 21 (1975).
[11]K. S. Liang, W. R. Salanek, and I. A. Aksay, Solid State Commun. 19, 329 (1976).
[12]R. S. Williams, S. P. Kowalczyk, P. S. Wehner, G. Apai, J. Stöhr, and D. A. Shirley, J. Electron Spectrosc. Relat. Phenom. 12, 477 (1977).
[13]P. H. Citrin, G. K. Wertheim, and Y. Baer, Phys. Rev. Lett. 41, 1425 (1978).
[14]P. H. Citrin and G. K. Wertheim, following paper, Phys. Rev. B 27, 3176 (1983).
[15]P. H. Citrin, G. K. Wertheim, and Y. Baer, Phys. Rev. B 16, 4256 (1977).
[16]J. R. Lloyd and S. Nakahara, J. Vac. Sci. Technol. 14, 655 (1977); S. Nakahara (private communication).
[17]Y. Baer, G. Busch, and P. Cohn, Rev. Sci. Instrum. 46, 466 (1975).
[18]W. Bambynek, B. Crasemann, R. W. Fink, H.-U. Freund, H. Mark, C. D. Swift, R. E. Price, and P. V. Rao, Rev. Mod. Phys. 44, 716 (1972).
[19]C. P. Flynn, Phys. Rev. Lett. 37, 1445 (1976). The calculated values here are qualitative but serve to justify our assumptions.
[20]S. Doniach, and M. Šunjić, J. Phys. C 3, 385 (1970).
[21]G. K. Wertheim and S. Hüfner, Phys. Rev. Lett. 35, 53 (1975).
[22]B. L. Henke, Phys. Rev. A 6, 94 (1972).
[23]M. Klasson, J. Hedman, A. Berndtsson, R. Nillson, C. Nordling, and P. Melnick, Phys. Scr. 5, 93 (1972).
[24]F. R. McFeely, J. Stöhr, G. Apai, P. S. Wehner, and D. A. Shirley, Phys. Rev. B 14, 3273 (1976).
[25]T.-C. Chiang and D. E. Eastman, Phys. Rev. B 23, 6836 (1981).
[26]S. Evans, R. G. Pritchard, and J. M. Thomas, J. Phys. C 10, 2483 (1977).
[27]D. R. Penn, J. Electron Spectrosc. Relat. Phenom. 9, 29 (1976).
[28]A. Barrie and N. E. Christensen, Phys. Rev. B 14, 2442 (1976).
[29]G. K. Wertheim and P. H. Citrin, in *Photoemission in Solids I,* Vol. 26 of *Topics in Applied Physics,* edited by M. Cardona and L. Ley (Springer, Heidelberg, 1978), p. 197.